Safety Considerations of an Unignited Hydrogen Release from Onboard Storage in a Naturally Ventilated Covered Car Park

Hussein H.G., Brennan S.*, Makarov D., Shentsov V., Molkov V.

[1] *Hydrogen Safety Engineering and Research Centre (HySAFER), Ulster University, Shore Road, Newtownabbey, BT37 0QB, UK*
**Corresponding author's email: sl.brennan@ulster.ac.uk*

ABSTRACT

Unignited hydrogen release from 700 bar onboard storage in a naturally ventilated covered car park has been simulated and analysed. A typical car park with dimensions LxWxH=30x28.6x2.6 m was considered. The car park had two vents of equal area on opposing walls: front and back to facilitate cross-flow ventilation based on the British standard (BS 7346-7:2013). Each vent had an area equal to 2.5% of the car park floor area, in line with BS 7346-7:2013 and similar international standards. Releases through three different Thermally Activated Pressure Relief Devices (TPRD) diameters of 3.34, 2.00 and 0.50 mm were compared, to understand the gas dispersion, specifically the dynamics of the flammable envelope (4% vol H_2), and envelopes of 1% and 2% H_2 as these are relevant to sensor and ventilation system activation as required by NFPA 2 standard for enclosures. Concentrations in the vicinity of the vehicle and of the vents are of particular interest. A blowdown model developed in Ulster University was applied to simulate realistic scenarios, and a comparison between an idealistic constant flow rate release and blowdown through a 3.34 mm TPRD diameter highlighted the conservative nature of a constant flow rate release. However, even accounting for the blowdown demonstrated that a release through a TPRD diameter of 3.34 mm leads to the formation of a flammable cloud throughout the majority of the carpark space in less than 20 s. Such a flammable envelope is not observed to the same extent for a TPRD diameter of 2 mm and the flammable envelope is negligible for a 0.5 mm diameter TPRD. Based on ISO/DIS 19880-1, NFPA 2 and IEC (60079-10) standards for equipment with gaseous hydrogen, the ventilation system must work to maintain hydrogen concentration under 1% of hydrogen mole fraction in the air, above this there should be ventilation sensor activation. Whilst a release through a 2 mm TPRD diameter resulted in concentrations of 1% hydrogen along the length of the car park ceiling within 20 s, in contrast an upward release through a 0.5 mm diameter led to concentrations of 1% reaching a very limited area of the ceiling. The simulations comparing an upward and downward release through a 0.5 mm TPRD demonstrated the effect of release direction on hydrogen dispersion. However, this effect is not as pronounced as the effect of changing TPRD diameter. It can be concluded that onboard vehicle storage with a TPRD diameter of 0.5 mm appears to be inherently safer for the scenario considered, as opposed to "typical" larger diameter TPRDs which the study indicates should be carefully investigated to ensure safety in a naturally ventilated covered car park.

KEYWORDS: Unignited release, covered carpark, hydrogen safety, indoor dispersion, natural ventilation.

INTRODUCTION

The number of hydrogen-powered vehicles on the market is growing and it is important to ensure they are at least as safe as conventional vehicles. Onboard hydrogen is typically stored as a compressed gas under high pressure (35 MPa for buses and 70 MPa for cars) and storage tanks are fitted with Thermally Activated Pressure Relief Devices (TPRD) to release hydrogen, avoiding tank rupture when the surrounding temperature reaches 110°C or above. In the event of a TPRD

Proceedings of the Ninth International Seminar on Fire and Explosion Hazards (ISFEH9), pp. 1407-1421
Edited by Snegirev A., Liu N.A., Tamanini F., Bradley D., Molkov V., and Chaumeix N.
Published by Saint-Petersburg Polytechnic University Press
ISBN: xxx-xxx-xx-xxxx-x :: DOI: 10.18720/spbpu/2/k19-27

activation, the released hydrogen might not ignite, instead of forming a flammable atmosphere and an explosion may occur in the presence of an ignition source. The potential delayed ignition and explosion event will not be explored in this study which instead focuses on release and dispersion. Failure of a TPRD or a fire on the opposite side of the tank has potential to cause an unignited release, it is this potential unignited release from a TPRD, in a covered car park which is discussed here. By necessity, hydrogen vehicles will be parked indoors, in garages, underground car parks, and present in tunnels, etc. Unignited hydrogen releases in an enclosure have been covered in the literature to a certain extent. However, with the exception of the work by Houf et al. [1], who considered releases from forklifts in warehouses, to date, the emphasis of numerical studies has tended towards low release rates and/or smaller enclosures. For instance, Venetsanos et al. [2] undertook an inter-comparison of CFD models in 2009 to investigate the model capability to reproduce hydrogen dispersion in a garage for a 1 g/s release from a 20 mm leak diameter in a 78.38 m^3 enclosure with two 5 cm diameter vents on one wall. In 2010, Papanikolaou et al. [3] assessed numerically the ventilation requirements for a residential garage with onboard hydrogen storage. In 2013, Bernard-Michel et al. [4] performed an inter-comparison of CFD models for a 4 Nl/min helium release in a 1 m^3 enclosure with 1 cm circular vent at the base of one wall. Molkov and Shentsov [5] validated the CFD model for buoyant hydrogen releases against the experimental study of Cariteau and Tkatschenko [6] for a small laboratory scale enclosure. When considering unignited releases in an enclosure, both the concentration decay and overpressure may be of interest. Free jets have been previously studied at Ulster and a nomogram is presented in Molkov [7, 8] to calculate hydrogen concentration decay in a jet. Li et al. [9] numerically investigated unignited and ignited releases from a 4.2 mm diameter TPRD under the car in the open air and it was concluded that the hazard distance for the unignited releases was somewhat longer than those for the ignited release. Previous numerical and analytical work by the authors on unignited releases indoors have been focused on momentum-dominated releases in enclosures with minimum ventilation, leading to the pressure peaking phenomenon [10-13]. However, in order for pressure peaking phenomenon to occur the release and enclosure geometry must be such that no air ingress occurs into the enclosure. Whilst this is relevant to residential garages, pressure peaking will not be caused by releases from typical TPRD diameters in car parks with the minimal ventilation legally required. To date, little or no publications exist on hydrogen unignited releases in car parks.

Ventilation recommendations exist to minimise the potential formation of a flammable atmosphere within an enclosure. Ventilation systems should be able to keep hydrogen concentration below the lower flammability limit (LFL) of 4% vol in order to eliminate potential ignition and flame propagation with pressure build up. Indeed, standards typically recommend concentrations do not exceed fractions of the LFL. Standards ISO/DIS 19880-1 [14], NFPA 2 [15] and IEC (60079-10) [16] require that the ventilation rate should ensure a maximum hydrogen mole fraction at 25% of the LFL for enclosures and buildings containing hydrogen equipment, i.e. 1% vol in the case of hydrogen. As an increasing number of car parks are built the majority are constructed in the basement of residential and commercial buildings [17]. In the literature, both underground car parks and those with two or more sides and a roof are referred to as covered car parks. Previous studies have focused on car fires in a car park and the amount of heat released from such a fire [18]. For example, the smoke movement and fire spread were numerically investigated by Zhang et al. [19] for an underground car park containing three burning cars. Joyeux et al. [20] indicated that the majority of fires in covered car parks involve only one car with the exception of the Schiphol fire accident, where around 10 to 30 cars were engulfed with fire. The difference in ventilation approaches should also be noted, with only wind and buoyancy the influencing factors where natural ventilation is considered. There are no existing studies, either experimental or numerical investigating safety aspects of an unignited hydrogen release in a large confined space such as a naturally ventilated covered car park. The release of hydrogen through a TPRD, dispersion and potential accumulation should be investigated to understand the potential hazards, helping to

address potential safety issues. Such an investigation is necessary and in the public interest and hence is the subject of this paper.

PROBLEM DESCRIPTION

This work focuses on an unignited hydrogen release in a naturally ventilated covered car park. CFD is used to provide insight into the flow process, including the prediction of flammable zone formation, temperature gradient, and flow patterns inside the covered car park. A typical covered car park has been simulated with dimensions of LxWxH=30x28.4x2.6 m as can be seen in Fig. 1 (ceiling is not shown). The car park has two ventilation openings: a back vent and front vent. They have an equal area but differ in shape. The front vent consists of a top to the bottom opening to drive through and two smaller connected side vents near the car park ceiling, representing an area typical of "door with two side vents". In contrast, the back vent is located on the top centre of the back-wall opposite to the front vent. The ventilation requirements were accounted for based on British Standard BS 7346-7:2013 [21] where it is recommended that a covered car park with natural ventilation should have an opening area equivalent to 5% of the floor area for each floor in a level. Similarly, the standard in the Netherlands NEN 2443 [22], requires vents area equivalent to 2.5% of the floor area on each opposite wall (5% in total). Thus, the two vents considered were of equal area (21.45 m^2) and located on opposite walls.

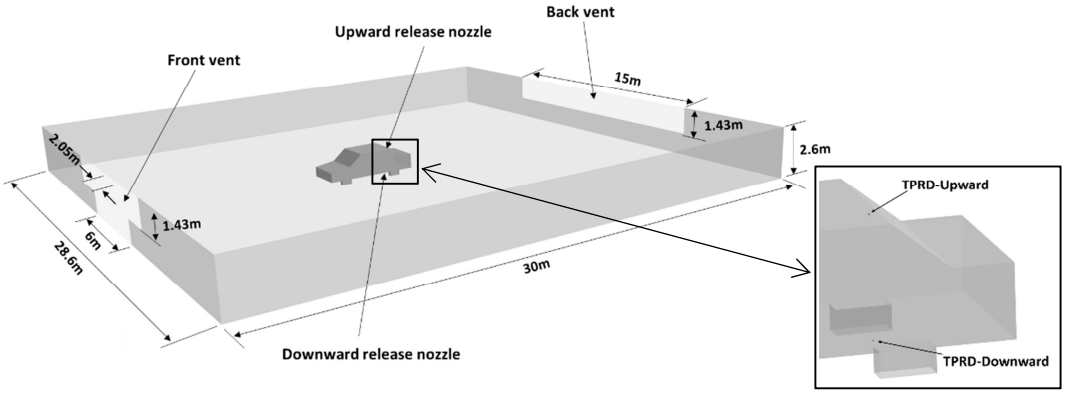

Fig. 1. Sketch of the naturally ventilated covered carpark with car geometry. Insert highlights TPRD location.

Six scenarios were considered by varying TPRD diameters and release type, these are listed in Table 1. The under-expanded jet theory developed at Ulster University [23] was used to calculate the equivalent diameter for the leak inlet (notional nozzle), thus avoiding the need to resolve the shock structure of the real jet at the TPRD exit. The car volume was not considered in 4 of the 6 cases. This allowed a safer diameter to be determined independent of car geometry. The release in these cases was located exactly at the centre of the car park at a position 0.5 m above the floor. However, a car geometry was considered for two scenarios with a release through a 0.5 mm TPRD diameter where release direction and position on the car was assessed. A typical saloon car with dimensions of 4.9 m length, 1.88 m width, and 1.47 m height was chosen. It was assumed that the car was stationary at the time of the leak and the onboard hydrogen tank was filled to capacity. This allows investigation of the worst case scenario. The hydrogen tank was assumed to have a volume of 117 litres and storage pressure of 70 MPa, with a capacity of approximately 5 kg. It was assumed that the car body is 0.25 m above the ground, with "square" wheels representing the actual equivalent circular diameter.

There are two possibilities for TPRD location: underneath the car close to the rear left the wheel or

the upper rear of the car close to back windshield facing upwards. These two scenarios have been considered in this study and it was assumed that both were located to the left side of the car with the same horizontal coordinates but differing height, (1.47 and 0.25 m from the floor respectively). The centre of the leak was situated in the centre of the car park, meaning the car body was positioned slightly left of centre. The ambient temperature and pressure were taken as 293 K and 101325 Pa respectively, and the fully quiescent conditions were considered, i.e. no wind effects, replicating a car park located in an urban setting. It is noted that a TPRD release is likely to result in an ignited release when it is triggered by a high temperature, and this is the subject of ongoing studies by the authors. However, the malfunction of a TPRD or activation through impact, warrants investigation, particularly with standard ventilation requirements based on gas concentrations.

Table 1. Scenarios considered for unignited hydrogen release in a naturally ventilated covered car park

Case number	Real release diameter (Notional nozzle diameter) (mm)	Release direction	Car geometry	Blow-down model	Hydrogen mass flow rate (kg/s)
1	3.34 (56.4)	Upward	No	No	0.2993
2	3.34 (56.4)	Upward	No	Yes	0.2993
3	2 (33.8)	Upward	No	Yes	0.1072*
4	0.5 (8.44)	Upward	No	Yes	0.0067*
5	0.5 (8.44)	Upward	Yes	Yes	0.0067*
6	0.5 (8.44)	Downward	Yes	Yes	0.0067*

* Value at the initial stage, before blow down.

MODEL AND NUMERICAL APPROACH

Overview

The CFD package ANSYS Fluent [24] was the base software tool used to simulate this high-pressure hydrogen release scenario. Whilst this study is timely and needed to inform the development of RCS, no previous work exsists on hydrogen releases in carparks, and as such there is no experimental data. Indeed there is limited experimental data for high pressure impinging hydrogen jets at a large scale. Indeed it is hoped that this work can thus assist in addressing hydrogen safety issues regarding large size enclosures with vents. ICEM CFD was used to generate the geometries and hexahedral meshes, with ANSYS Fluent to solve the governing equations. A pressure-based solver has been used and PISO (Pressure Implicit with the Splitting of Operators) was applied in this study for transient flow calculations. The compressible flow was considered, and second-order upwind schemes have been used for all spatial discretisation, with the exception of the pressure gradient where the PRESTO! interpolation method was applied. A least-squares cell-based approach was used for interpolation methods (gradients). Heat transfer by conduction, convection, and radiation was accounted for as described in previous work by the authors [10, 25].

Governing equations

The Reynolds-Average Navier-Stokes (RANS) conservation equations were considered solving mass, momentum, energy, and species,

$$\frac{\partial \bar{\rho}}{\partial t} + \frac{\partial \bar{\rho}\tilde{u}_j}{\partial x_j} = S_{mass}, \quad (1)$$

$$\frac{\partial(\bar{\rho}\tilde{u}_i)}{\partial t}+\frac{\partial(\bar{\rho}\tilde{u}_i\tilde{u}_j)}{\partial x_j}=-\frac{\partial\bar{p}}{\partial x_i}+\frac{\partial}{\partial x_j}(\mu+\mu_t)\left(\frac{\partial\tilde{u}_i}{\partial x_j}+\frac{\partial\tilde{u}_j}{\partial x_i}-\frac{2}{3}\delta_{ij}\frac{\partial\tilde{u}_k}{\partial x_k}\right)+\bar{\rho}g_i, \quad (2)$$

$$\frac{\partial(\bar{\rho}\tilde{E})}{\partial t}+\frac{\partial}{\partial x_j}\left(\tilde{u}_j(\bar{\rho}\tilde{E}+\bar{p})\right)=\frac{\partial}{\partial x_j}\left(\left(k+\frac{\mu_t\,c_p}{Pr_t}\right)\frac{\partial\tilde{T}}{\partial x_j}-\sum_m\tilde{h}_m\left(-\left(\rho D_m+\frac{\mu_t}{Sc_t}\right)\frac{\partial\tilde{Y}_m}{\partial x_j}\right)+\tilde{u}_i\,(\mu+\mu_t)\left(\frac{\partial\tilde{u}_i}{\partial x_j}+\frac{\partial\tilde{u}_j}{\partial x_i}-\frac{2}{3}\frac{\partial\tilde{u}_k}{\partial x_k}\,\delta_{ij}\right)\right)+S_E, \quad (3)$$

$$\frac{\partial(\bar{\rho}\,\tilde{Y}_m)}{\partial t}+\frac{\partial}{\partial x_j}\left(\bar{\rho}\tilde{u}_j\tilde{Y}_m\right)=\frac{\partial}{\partial x_i}\left[\left(\bar{\rho}D_m+\frac{\mu_t}{Sc_t}\right)\frac{\partial\tilde{Y}_m}{\partial x_j}\right]+R_m+S_m, \quad (4)$$

where t is the time, ρ is the density, k represents turbulence kinetic energy, μ_t is the turbulent dynamic viscosity, p is the pressure, S_{mass} is the source term which can be added by user define function (UDF), u represents the velocity components, E is the total energy, δ_{ij} is the Kronecker symbol, c_p is the specific heat at constant pressure, g_i is the gravitational acceleration, Sc_t and Pr_t are the turbulent Schmidt and energy turbulent Prandtl numbers, which are 0.7 and 0.85 respectively, Y_m is the mass fraction, D_m is the molecular diffusivity of the species m, S_E are the source terms in the energy equation, R_m and S_m are the net production/consumption rate by species m chemical reaction and the source term connected to any functions defined by the users for dispersed phase.

Turbulence model

The realizable *k-ε* turbulent model [25] was considered to solve the transport equation for turbulence kinetic energy (k) and turbulent dissipation rate (ε):

$$\frac{\partial(\rho k)}{\partial t}+\frac{\partial}{\partial x_i}(\rho k u_i)=\frac{\partial}{\partial x_i}\left[\left(\mu+\frac{\mu_t}{\sigma_k}\right)\frac{\partial k}{\partial x_i}\right]+G_k+G_b-\rho\,\varepsilon-Y_m+S_k, \quad (5)$$

$$\frac{\partial(\rho\,\varepsilon)}{\partial t}+\frac{\partial}{\partial x_i}(\rho\varepsilon u_i)=\frac{\partial}{\partial x_i}\left[\left(\mu+\frac{\mu_t}{\sigma_\varepsilon}\right)\frac{\partial\varepsilon}{\partial x_i}\right]+\rho C_1 S\varepsilon-\rho C_2\frac{\varepsilon^2}{k+\sqrt{v\varepsilon}}-C_{1\varepsilon}\frac{\varepsilon}{k}C_{3\varepsilon}\,G_b+S_\varepsilon, \quad (6)$$

where, Y_m is the contribution of the fluctuating dilatation in compressible turbulence to the overall dissipation rate, G_b and G_k are the buoyancy and the mean velocity gradient respectively, which presents the k generation, v is the kinematic viscosity, σ_k and σ_ε are the Prandtl numbers of turbulence for k and ε, corresponding to 1 and 1.2. $C_{3\varepsilon}$ is calculated as a function of the flow velocity components with respect to the gravitational vector while C_2 and $C_{1\varepsilon}$ are constants 1.90 and 1.44 respectively. C_1 is evaluated as a function of the modulus of the mean rate of the strain sensor, S. S_k is a source term to be defined by User Define Function (UDF) for Turbulence Kinetic Energy while S_ε represents a UDF source term for turbulence dissipation rate, which was calculated from blowdown parameters via a UDF in this study. This model outperforms the standard κ-ε model especially for calculating spreading rate in axisymmetric jets [24,27].

Boundary and initial conditions

A domain with outer dimensions 170x 128.6 x 92.6 m (LxWxH) was used, which is axisymmetric lengthwise. A hexahedral mesh was generated throughout the domain, details of which are given later in this paper. The walls were not meshed in depth. The car park floor, walls, and the roof had a thickness of 0.15 m and were assumed to be constructed of concrete, and the release pipe or car body was considered to be made of aluminium. The material properties chosen are similar to concrete typically used for car parks in the UK. Two materials were used in this study: aluminium and concrete, and the details of the material properties can be found in a previous publication [25]. A box mesh technique with mesh interfaces was implemented to provide a refined mesh around the nozzle and inside the car park, making it possible to improve resolution without a significant increase in total number of control volumes. A no-slip condition was applied at the solid surfaces.

The domain was assumed to be initially 100% air at normal ambient pressure and temperature (101325 Pa and 293 K respectively).

Notional nozzle model and blowdown process

Hydrogen released from a 70 MPa tank through a TPRD forms an under-expanded jet, leading to a complex shock structure at the nozzle exit, which is computationally intensive to capture. It is not necessary to solve this shock structure in this work as it is not the focus of this study. Therefore, the notional nozzle theory developed by Molkov et al. [23] and described in detail in [8] has been applied. In addition, their blowdown model was implemented. Molkov et al. [23], found that the adiabatic blowdown model provided better agreement with experiment than an isothermal approach for the initial stage whilst the isothermal blowdown model provided better agreement compared to experimental data for high-pressure hydrogen storage (930 bar) in later stages in case of release temperature prediction as studied by Cirrone et al. [28] . Thus, an adiabatic model has been used in this study to reproduce the hydrogen tank blowdown since only the initial stage of the blowdown process was considered. Predicted pressure dynamics for blowdown through 3.34 mm, 2 mm and 0.5 mm diameters are shown in Fig. 2.

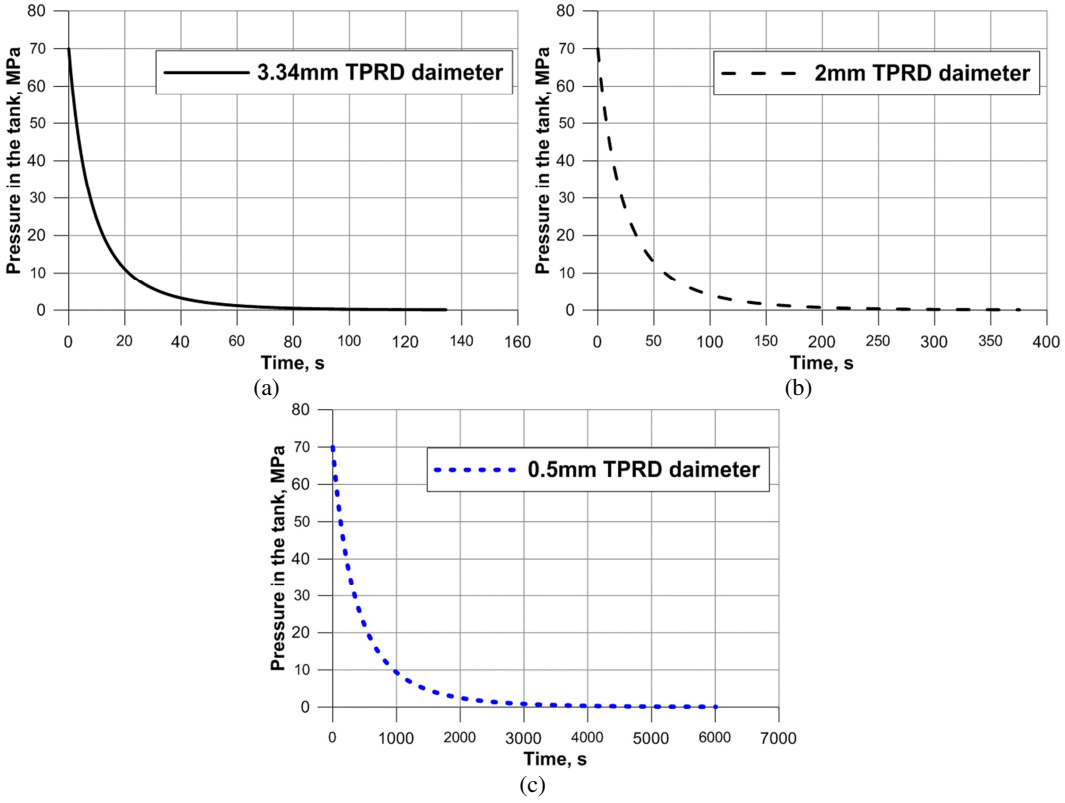

Fig. 2. Tank pressure for adiabatic blowdown from 70 MPa. (a) 3.34 mm diameter TPRD; (b) 2 mm diameter TPRD; (c) 0.5 mm diameter TPRD.

When the TPRD diameter is 3.34 mm for a 117 L tank at 70 MPa, the total blowdown takes over 138 s and the transition from under-expanded jet to expanded jet occurs at 106 s. In contrast, a 0.5 mm diameter TPRD requires 6000 s to fully blowdown and 4742 s to transit to an expanded jet. These differences have to be accounted for by hydrogen tank designers as they affect the required thermal resistance of tank to a fire. It is acknowledged that this presents a significant engineering

challenge. Redesign of ventilation systems is also an option. However, this would not eliminate problems associated with ignited releases and vehicles would be restricted to use in enclosures that had been retrofitted or newly designed, rather than ensuring all uses are inherently safe.

Volumetric source model

Decreasing tank pressure during blowdown leads to a corresponding reduction in the notional nozzle diameter. In order to avoid constantly changing the release diameter in the CFD calculation, a volumetric source approach [23] was implemented in a single cell above the leak. This mimics the hydrogen mass inflow by taking mass, momentum, energy, turbulent kinetic energy and turbulent dissipation energy data from written for Fluent the User Defined Function (UDF). This approach enables changes in the notional nozzle parameters to be reflected in the volumetric sources without any change in the release shape and volume. This method was experimentally validated for hydrogen releases through a 3 mm diameter [29] and the results were presented in detail in [23]. It was demonstrated that a volumetric source equivalent to 4 times (or less) the notional nozzle diameter can accurately reproduce concentration decay in the under-expanded jets. All volumetric sources used in this study are either equal to or larger than the notional nozzle diameter.

Grid independency

In order to comply with the CFD model evaluation protocols [30], three different grids were considered (coarse, intermediate, and refined). In each grid refinement, the average length of the computational cells was halved inside the car park, particularly in areas where high gradients and complex phenomena were expected. Specifically, localised refinement was provided around the hydrogen inlet, the ceiling and regions of the enclosure volume for all grids as recommended by Baraldi et al. [30]. The study was conducted for case 1 and the mesh details are summarised in Table 2.

Table 2: Mesh details for grid independence study

Mesh size	No. of cells	No. of faces	No. of nodes
1. Coarse	479,977	1,639,600	532,532
2. Intermediate	691,759	2,302,631	745,416
3. Refine	1,222,412	3,978,771	1,296,276

It should be noted that only the mesh within the car park was changed in this grid independence study since the outer domain does not effect conditions in the initial stages of the release. The hydrogen mole fraction was measured at points along the jet axis at increasing height relative to the release, results from a flow time of 0.7 s are shown in Fig. 3a. In addition, concentrations were recorded for points 0.021 m under the car park ceiling at an increasing radius from the jet axis, these results at 0.7 s are shown in Fig. 3b.

As seen in Fig. 3b the hydrogen cloud has a radius of 4m at 0.7 s. The grid independence study showed no significant changes in the results when a coarser grid is used, yet significant savings were made in computational time. Therefore, an “intermediate grid”, as described in Table 2 was used in the study to achieve a balance between accuracy and computational time.

MODEL VALIDATION

As discussed, no exsisting experimental data exsists for a hydrogen release in a covered car park, and limited data exsists for impinging uignited jets. However, experimental data for impinging helium jets, produced by KIT-HYKA has been considered for comparison. The experiments were

carried out within the H2FC European Infrastructure project (http://www.h2fc.eu/) and have not been published in their entirety, however, they are summarised in the work by Dadashzadah et al. [31]. The experiments involved blowdown from a 19 l tank at 70 MPa through a release diameter of 1 mm. The release occurred vertically and impinged on to a plate with dimensions 1.52 x 1.51 m. The plate was located 85 cm from the release point. Helium concentration was was measured at locations along the surface locations. Two sensors were considered for validation purposes, as shown in Fig. 4. Pos 1 was located at a distance of 100 mm distance from the jet axis, and Pos 2 was located 250 mm from the jet axis. on the exact axis as the first one. Two steps were taken in the validation process; blowdown parameters were compared with those predicted by the Ulster blowdown model, then these validated pressure dynamic curves were used as an input to the CFD simulation.

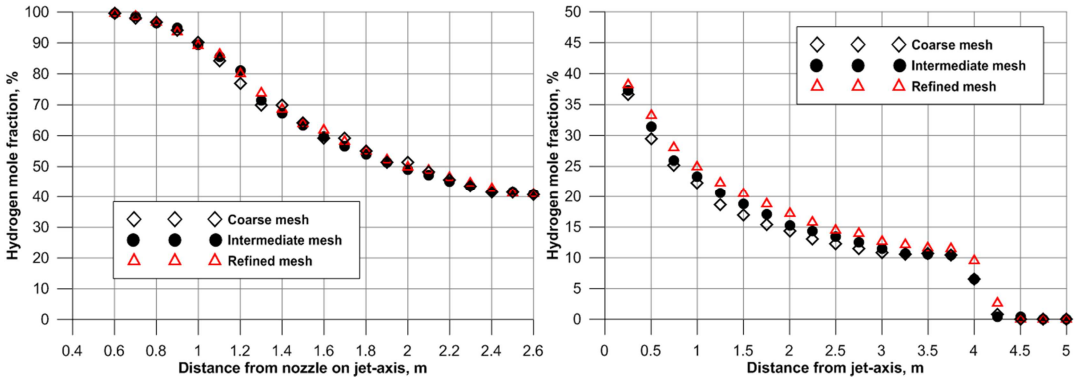

(a) (b)

Fig. 3. Grid independence study for 3.34 mm TPRD diameter with constant release (case 1) at a flow time of 0.7 s. (a) Hydrogen mole fraction at increasing vertical distance from the leak nozzle along jet axis; (b) Hydrogen mole fraction at increasing radial distance from the jet axis at a position 0.021 m under the car park ceiling.

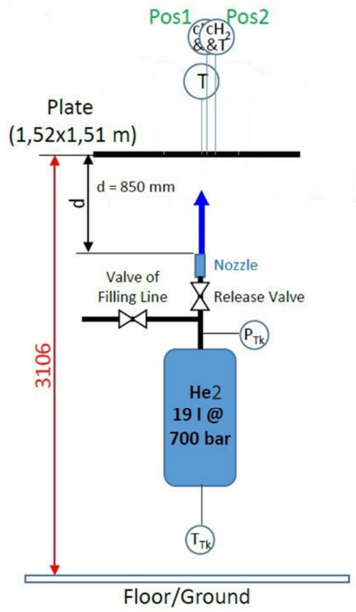

Fig. 4. Schematic diagram of KIT experiment for an impinging helium jet.

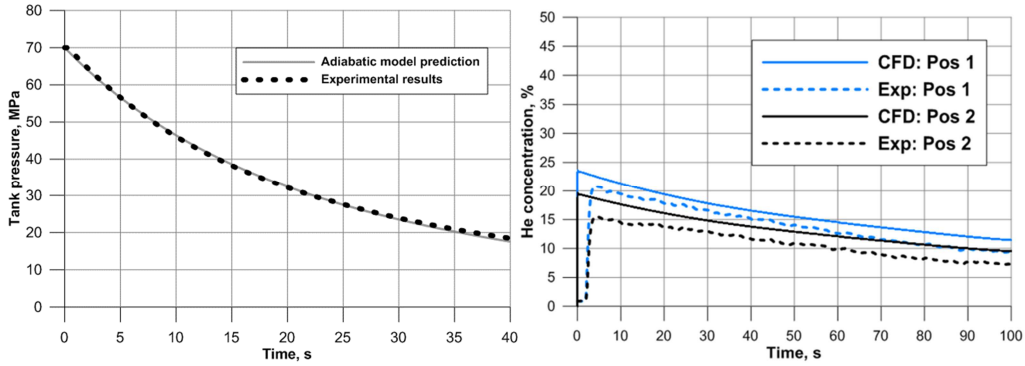

Fig. 5. Experimental and numerical predictions. (a) Storage pressure dynamics ; (b) Helium concentration at plate surface sensors

Experimentally measured pressure dynamics at the release point were compared with those predicted using the Ulster adiabatic blowdown model with a Discharge Coefficient (C_D) of 0.8. Good agreement was found between the model predictions and experiment as shown in Fig. 5a.

A volumetric source model was employed for the helium release in the CFD simulations. A hexahedral grid was used with refinement in the region of the nozzle area and plate. An indoor environment was considered with dimensions of L x W x H of (25.32 x 7.87 x 10.42) m. A comparison of the concentraion measurements at Pos 1 and Pos 2 is given in Fig 5b. Differences are within allowable engineering limits, with differences observed of 10 to 12%. It should be noted that in the experiments, in order to measure concentration, helium gas was suctioned at the plate surface to a helium measuring device along an 80 cm tube, this may be a factor in the time delay observed between the experimental measurements at the beginning of the experiment. Differences between the numerical prediction and the experiment decreased with increasing time.

RESULTS

Previous studies by the authors have focused on unignited and ignited hydrogen release in small laboratory-scale enclosures and residential garages to evaluate TPRD diameters, vent position, and size, to avoid the safety risk due to the pressure peaking phenomena [10]. Whereas in this work the larger vents mean that overpressure is not the most significant hazard. Thus, the focus of this work is on the development of a flammable atmosphere for the six cases, with a specific emphasis on 1% vol as this represents the maximum allowable mole fraction of hydrogen in an enclosure containing hydrogen equipment in accordance to ISO/DIS 19880-1 [14], NFPA 2 [15] and IEC (60079-10) [16] standards and guidelines

Development of flammable atmosphere for constant hydrogen release

A constant hydrogen release of 0.299 kg/s through a 3.34 mm TPRD diameter as simulated in [24] was considered. Current TPRD diameters can range from 2 to 5 mm and 3.34 mm was taken as the largest diameter in this study. Whilst this facilitates tank blowdown in a shorter period of time and decreases the risk of tank rupture, the hazards for indoor release, where the gas may accumulate should be considered. This case represents the worst case scenario considered in this study as blowdown is not accounted for. However, accumulation is evident within the first seconds of the release before the pressure drop in a blowdown scenario would be significant. It is also indicative of what may occur in the event of leaks from other compressed hydrogen gas sources, where pipes and tanks may have a leak with a constant release of hydrogen flow for a longer period. Dispersion of

hydrogen over the first 20 s of the release can be seen in Fig. 6, the iso-surfaces show the extent of the flammable atmosphere (4% vol), and of 25% the LFL (1% vol). Where 1% vol represents the maximum allowable mole fraction of hydrogen in an enclosure containing hydrogen equipment in accordance to ISO/DIS 19880-1 [14], NFPA 2 [15] and IEC (60079-10) [16] standards and guidelines.

It can be seen from Fig. 6 that within just 20 s hydrogen concentration is 1% vol or higher throughout the enclosure, demonstrating that for the particular release, the natural ventilation of the car park is incapable of maintaining a hydrogen mole fraction below 1%, any hydrogen sensors present would be activated. It can also be seen how a flammable atmosphere has been formed across almost the entire ceiling of the carpark and around the ventilation openings within just 20 s of release. Whilst this is a worst case scenario it does highlight potential safety concerns which should be taken into account by engineers.

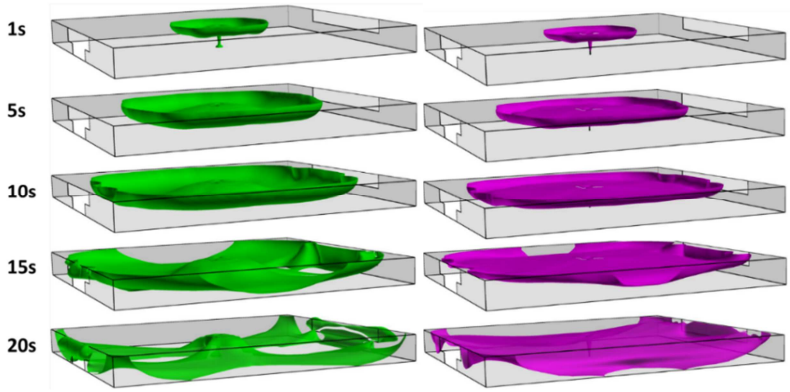

Fig. 6. Hydrogen mole fraction for a constant release of 0.299 kg/s through a 3.34 mm diameter TPRD. (a) Iso-surface 1% vol; (b) Iso-surface 4% vol.

The effect of TPRD diameter on hydrogen dispersion in the car park

To reflect more realistic scenarios a blowdown model was implemented using the volumetric source as described in the previous sections. Three different (3.34 mm, 2 mm, 0.5 mm) TPRD diameters were considered and compared with the constant release from 3.34 mm TPRD diameter described previously. Iso-surfaces of 1% vol and 2% vol for the various TPRD diameters at 20 s can be seen in Fig. 7. In Fig. 8 Iso-surfaces of 4% vol for the various TPRD diameters at 20 s are shown representing the LFL. The effect of accounting for blowdown through the 3.34 mm TPRD can be clearly seen and is most evident in Fig. 8.

It can be seen that even when blowdown is accounted for a TPRD diameter of 3.34 mm can lead to safety concerns, with a flammable atmosphere being formed throughout the carpark. In contrast, it is shown how a release through a 2 mm diameter TPRD from 700 bar leads to a much smaller flammable hydrogen cloud around the release nozzle and under the ceiling. Concentrations of 1% vol, are predicted in the vicinity of the vents within 20 s. A 2 mm TPRD diameter led to a flammable cloud with a radius of approximately 5 m above the leak and underneath the ceiling.

A 0.5 mm TPRD diameter was also investigated and it can be seen from Fig. 9 how a flammable cloud is formed in a very limited area above the leak in contrast with the larger diameters considered. From Fig. 9 it can be seen how the extent of the flammable atmosphere remains almost constant over the initial 20 s of the of the release. Thus, a TPRD diameter of 0.5 mm could be considered as an inherently safer diameter for unignited hydrogen release from onboard storage in

this case. In contrast, the extent of the hydrogen cloud at 1% continues to grow over 20 s, as shown in Fig. 9.

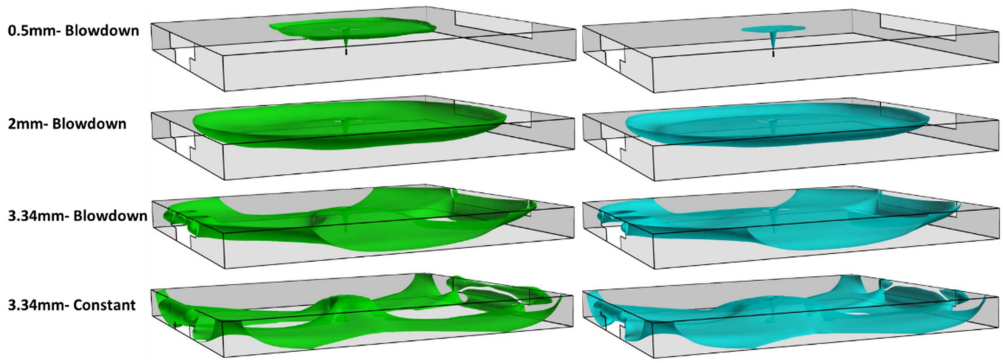

Fig. 7 Hydrogen mole fraction after 20 s for releases from 700 bar through 0.5 mm, 2 mm and 3.34 mm TPRD diameters. (a) Iso-surface 1% vol; (b) Iso-surface 2% vol.

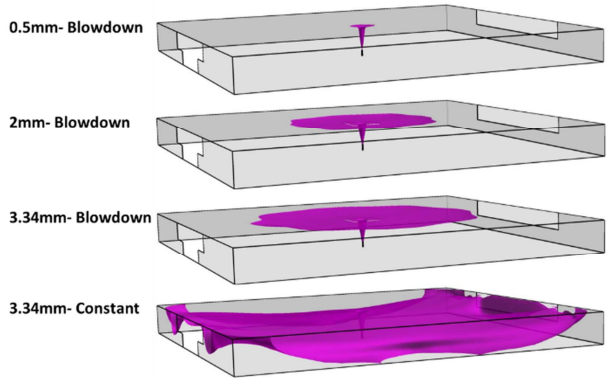

Fig. 8. Iso-surface showing 4% hydrogen mole fraction after 20 s for releases from 700 bar through 0.5 mm, 2 mm and 3.34 mm TPRD diameters.

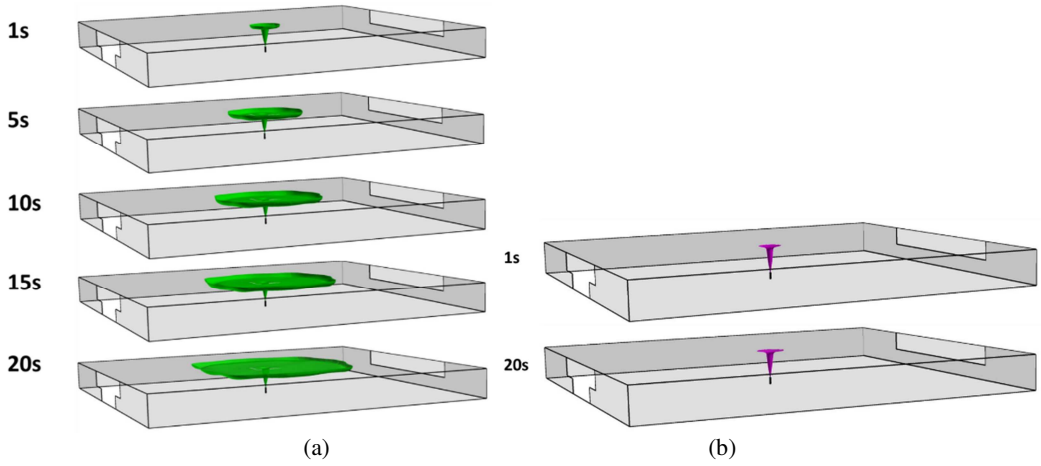

Fig. 9. Hydrogen mole fraction for a blowdown release from 700 bar through a 0.5 mm TPRD. (a) Iso-surface 1% vol; (b) Iso-surface 4% vol.

Hydrogen release direction from onboard storage in a naturally ventilated covered car park

In addition to releasing hydrogen through a "pipe" 0.5 m pipe above the car park floor, a car body was also considered to represent a more realistic scenario. Two different release directions were considered using a 0.5 mm TPRD diameter in order to investigate the effect of release orientation and release location. Results for a downward release, from a location under the car beside the rear left wheel, are shown in Fig. 10 for 4% hydrogen mole fraction.

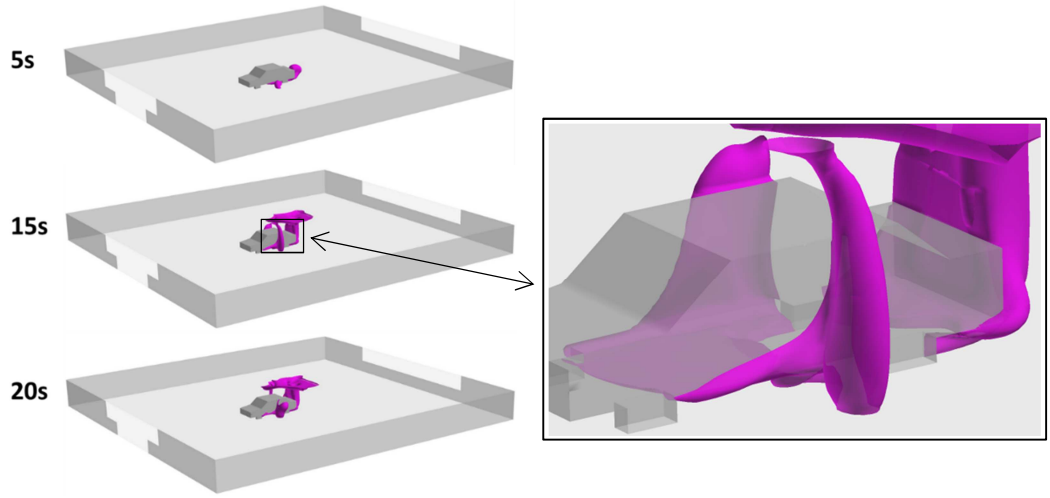

Fig. 10. Iso-surface showing 4% hydrogen mole fraction for a *downward* release from 700 bar through a 0.5 mm TPRD.

The maximum flammable envelope was reached at a release time of approximately 15 s, after which time the height of the jets at the sides and rear of the car began to reduce, this height reduction is observed by 20 s. Since the release was downwards, impinging on the floor, the car wheels obstructed some of the flow dispersion, leading to a non-uniform release pattern. H release. Within 15 s of the release, the flammable envelope covered the rear, left and right of the car in addition to regions of the ceiling. This presents a clear safety concern for any passengers in the car in the event ignition sources may be present. Nevertheless, the flammable cloud is relatively small and the hydrogen disperses quickly.

An upward release was also simulated at a height of 1.13 m from the ground, representing the top of the car and the results are shown in Fig. 11 for 4% hydrogen mole fraction.

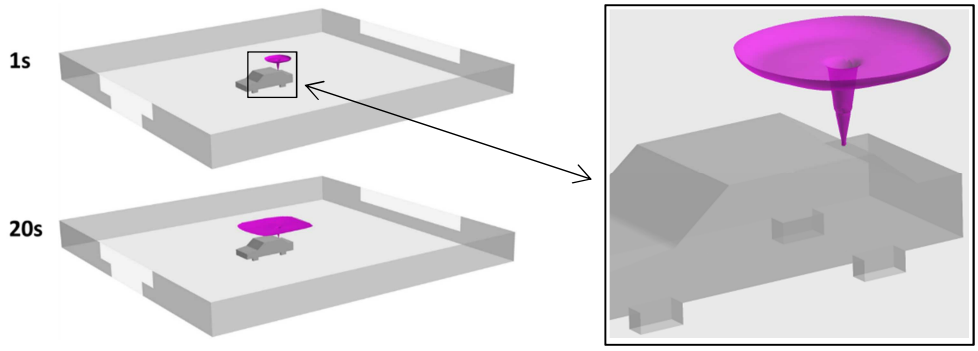

Fig. 11. Iso-surface showing 4% hydrogen mole fraction an *upward* release from 700 bar through a 0.5 mm TPRD.

For an upward release the maximum flammable envelope was formed at approximately 20 s, i.e. 5 s later than for the downward case. It can be seen from Fig. 11 how the flammable envelope covers a comparably larger area beneath the ceiling but is spread over a smaller region surrounding the car, and hence has a higher average hydrogen concentration.

A comparison of the gas envelope development for 1% hydrogen mole fraction for a downward and upward release through a 0.5 mm TPRD diameter is shown in Fig. 12. It is seen how for the downward release the envelope of 1% volume is considerably smaller in the region underneath the ceiling, however, the car itself is surrounded on three sides by the gas cloud at 1% hydrogen. In contrast, the upward release led to a relatively larger envelope of 1% hydrogen in the region beneath the ceiling, but a minimal envelope was seen in the vicinity of the car. It should be mentioned that both downward and upward releases could be classified as inherently safe if a 0.5 mm TPRD diameter is used because the flammable cloud produced is limited in a very small area, predominately near the ceiling, and it disperses quickly with continuing tank blowdown. However, TPRD diameters larger than 0.5 mm can lead to the more significant flammable cloud in the absence of additional ventilation. It should be emphasised that whilst the envelope at 1% vol has not reached a maximum at 1%, the flammable zone has already begun to reduce by this time, as discussed in the previous section.

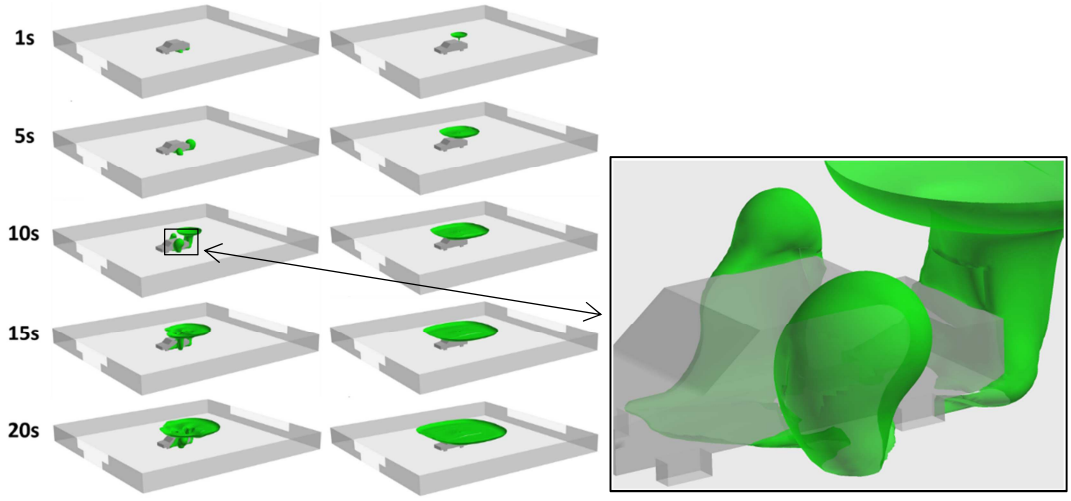

Fig. 12. Hydrogen release from 700 bar through a 0.5 mm TPRD. (a) Downward release; (b) Upward release.

CONCLUSIONS

Unignited hydrogen release from onboard vehicle storage in a naturally ventilated covered car park has been considered numerically for the first time. Simulations were carried out for a car park with dimensions LxWxH=30x28.6x2.6 m, incorporating two vents which provided an opening equivalent in area to 5% of the floor area across two opposing walls in accordance with British Standard BS 7346-7:2013. Six release cases from 700 bar storage were considered; four upward releases from a pipe 0.5 m above the floor, and a downward and upward release where the car geometry was included. A blowdown model, developed at Ulster University [23], was applied for all but one constant release scenario. As expected, a constant mass flow rate release resulted in a larger flammable cloud compared for a blowdown release through the same TPRD diameter, demonstrating the importance of including blowdown for real scenarios. It was demonstrated how a

0.5 mm diameter TPRD resulted in a considerably smaller flammable cloud. Concerns have been highlighted for ”typical” TPRD diameters and it has been demonstrated how the diameter should be reduced as much as is reasonably practicable. In order to investigate a real case scenario, a car body geometry was modelled, and downward and upward releases from 700 bar storage through a 0.5 mm TPRD were compared. The downward release resulted in a larger flammable envelope in the vicinity of the car, particularly surrounding the doors and rear. However, the average hydrogen concentration within the flammable cloud was lower compared with the upward release. In contrast, an upward release let to a greater flammable envelope beneath the ceiling, but not surrounding the car. Both downward and upward releases from 700 bar through a 0.5 mm TPRD in a covered car park can be considered as inherently safe producing a limited flammable cloud which disperses quickly. However, the work does indicate that if larger diameter TPRDs are to be used, then safety considerations for an unignited release in a covered car park should be further investigated and addressed.

REFERENCES

[1] W.G. Houf, G.H. Evans, I.W. Ekoto, E.G. Merilo, M.A. Groethe, Hydrogen fuel-cell forklift vehicle releases in enclosed spaces, Int. J. Hydrogen Energy 38 (2013) 8179-8189. doi:10.1016/j.ijhydene.2012.05.115.

[2] A.G. Venetsanos, E. Papanikolaou, M. Delichatsios, J. Garcia, O.R. Hansen, M. Heitsch, A. Huser, W. Jahn, T. Jordan, J.M. Lacome, H.S. Ledin, D. Makarov, P. Middha, E. Studer, A. V. Tchouvelev, A. Teodorczyk, F. Verbecke, M.M. Van der Voort, An inter-comparison exercise on the capabilities of CFD models to predict the short and long term distribution and mixing of hydrogen in a garage, Int. J. Hydrogen Energy 34 (2009) 5912-5923. doi:10.1016/j.ijhydene.2009.01.055.

[3] E.A. Papanikolaou, A.G. Venetsanos, M. Heitsch, D. Baraldi, A. Huser, J. Pujol, J. Garcia, N. Markatos, HySafe SBEP-V20: Numerical studies of release experiments inside a naturally ventilated residential garage, Int. J. Hydrogen Energy 35 (2010) 4747-4757. doi:10.1016/j.ijhydene.2010.02.020.

[4] G. Bernard-Michel, B. Cariteau, J. Ni, S. Jallais, E. Vyazmina, D. Melideo, CFD Benchmark Based Exp. Helium Dispers. a 1 M3 Enclos. e Intercomparisons Plume, In: Proceedings of ICHS 2013, Brussels, Belgium, 2013: p. paper ID No. 145.

[5] V. Molkov, V. Shentsov, Numerical and physical requirements to simulation of gas release and dispersion in an enclosure with one vent, i Int. J. Hydrogen Energy 39 (2014) 13328-13345. doi:10.1016/j.ijhydene.2014.06.154.

[6] B. Cariteau, I. Tkatschenko, Experimental study of the effects of vent geometry on the dispersion of a buoyant gas in a small enclosure, Int. J. Hydrogen Energy 38 (2013) 8030-8038. doi:10.1016/j.ijhydene.2013.03.100.

[7] V. Molkov, Hydrogen non-reacting and reacting jets in stagnant air: overview and state of the art, Proceedings of the 10th International Conference on Fluid Control, Measurement, and Visualization (FLUCOM2009), 17-21 August 2009. Moscow, Russia.

[8] V. Molkov, Fundamentals of Hydrogen Safety Engineering I, www.bookboon.com, 2012.

[9] Z.Y. Li, D. Makarov, J. Keenan, V. Molkov, CFD study of the unignited and ignited hydrogen releases from TPRD under a fuel cell car, ICHS (2015), Paper No.322.

[10] S. Brennan, H. G. Hussein, D. Makarov, V. Shentsov, V. Molkov, Pressure effects of an ignited release from onboard storage in a garage with a single vent, Int. J. Hydrogen Energy (2018). https://doi.org/10.1016/j.ijhydene.2018.07.130.

[11] S. Brennan, V. Molkov, Safety assessment of unignited hydrogen discharge from onboard storage in garages with low levels of natural ventilation, Int. J. Hydrogen Energy 38 (2013) 8159-8166. doi:10.1016/j.ijhydene.2012.08.036.

[12] D. Makarov, V. Shentsov, M. Kuznetsov, V. Molkov, Pressure peaking phenomenon: model validation against unignited release and jet fire experiments, Int. J. Hydrog. Energy 43 (2018) 9454-9469.

[13] S. Brennan, D. Makarov, V. Molkov, Dynamics of Flammable Hydrogen-Air Mixture Formation in an Enclosure with a Single Vent, Sixth Int. Semin. Fire Explos. Hazards. (2011) 978–981. doi:10.3850/978-981-08-7724-8.

[14] International Electrochnical commission IEC 60079-10-1, Explosive atmospheres – Part 10-1: Classification of areas - Explosive gas atmospheres, 2015.

[15] National fire protection association NFPA 2, Hydrogen technologies code, 2011.

[16] The International organization for standardization ISO/DIS 19880-1, Gaseous hydrogen – fuelling stations, Part 1: General requirements, 2018.

[17] W.K. Chow, On safety systems for underground car parks, Tunn. Undergr. Sp. Technol. (1998). doi:10.1016/S0886-7798(98)00060-1.

[18] M.G.M. van der Heijden, M.G.L.C. Loomans, A.D. Lemaire, J.L.M. Hensen, Fire safety assessment of semi-open car parks based on validated CFD simulations, Build. Simul. 6 (2013) 385–394. doi:10.1007/s12273-013-0118-7.

[19] X.G. Zhang, Y.C. Guo, C.K. Chan, W.Y. Lin, Numerical simulations on fire spread and smoke movement in an underground car park, Build. Environ. 42 (2007) 3466-3475. doi:10.1016/j.buildenv.2006.11.002.

[20] D. Joyeux, J. Kruppa, L.-G. Cajot, J.-B. Schleich, P. Van de Leur, L. Twilt, Demonstration of real fire tests in car parks and high buildings, Report EUR 20466, 2002.

[21] British Standard institution BS 7346-7:2013, Components for smoke and heat control systems – Part 7: Code of practice on functional recommendations and calculation methods for smoke and heat control systems for covered car parks, 2013.

[22] Nederlands Normalisatie-Instituut NEN 2443. parkeren en stallen van personenauto's op terreinen en garages, ICS 91.040.99, 2000.

[23] V. Molkov, D. Makarov, M. Bragin, Physics and modelling of underexpanded jets and hydrogen dispersion in atmosphere, In: Physics of Extreme States of Matter, 2009, pp. 146-149.

[24] ANSYS Fluent R16.2 User Guide, (2016).

[25] H. G. Hussein, S. Brennan, D. Makarov, V. Shentsov, V. Molkov, Numerical validation of pressure peaking from an ignited hydrogen release in a laboratory-scale enclosure and application to a garage, Int. J. Hydrogen Energy 43 (2018) 17954-17968.

[26] T.-H. Shih, W.W. Liou, A. Shabbir, Z. Yang, J. Zhu, A new k-ϵ eddy viscosity model for high Reynolds number turbulent flows, Comput. Fluids 24 (1995) 227–238. doi:10.1016/0045-7930(94)00032-T.

[27] S.B. Pope, An explanation of the turbulent round-jet/plane-jet anomaly, AIAA J. 16 (1978) 279-281. doi:10.2514/3.7521.

[28] D.M.C. Cirrone, D. Makarov, V. Molkov, Simulation of thermal hazards from hydrogen under-expanded jet fire. Int. J. Hydrogen Energy (2018).

[29] P.T. Roberts, L.C. Shirvill, T.A. Roberts, C.J. Butler, M. Royle, Dispersion of hydrogen from high-pressure sources, in: Inst. Chem. Eng. Symp. Ser., 2006, p. 410.

[30] D. Baraldi, D. Melideo, A. Kotchourko, K. Ren, J. Yanez, O. Jedicke, S.G. Giannissi, I.C. Tolias, A.G. Venetsanos, J. Keenan, D. Makarov, V. Molkov, S. Slater, F. Verbecke, A. Duclos, The CFD Model Evaluation Protocol, 2016.

[31] M. Dadashzadeh, D. Makarov, V. Molkov, Non-adiabatic blowdown model: a complementary tool for the safety design of tank-TPRD system, In: Proceedings of ICHS 2017, Hamburg, Germany, 2017.